Development of High Strength Hydroxyapatite for Hard Tissue Replacement

Sumit Pramanik[ξ], Avinash Kumar Agarwal[Ψ,*] and K.N. Rai [ξ]

[ξ]*Materials Science Programme*
[Ψ]*Department of Mechanical Engineering*
Indian Institute of Technology Kanpur
Kanpur-208016, India
[*]*Corresponding Author's Email: akag@iitk.ac.in*

Hydroxyapatite (HAp) is a suitable bioceramic material for hard tissue replacement. In this present work HAp has synthesized by solid state reactions in temperature near 1250^{o}C and it exhibits hexagonal crystal structure. HAp samples exhibited improvement in mechanical properties with increasing cold compaction pressure as well as recrushing operation. It also showed high resistance to surface reaction with the simulated body fluid. Surface morphology, pore volume, and particle size of the material have studied by Scanning Electron Microscopy, Brunauer-Emmett-Teller technique, and Particle Size Analysis. Chemical bonding present in the newly produced hydroxyapatite material was confirmed by Fourier Transform Infrared Spectrometry.

Introduction

Hydroxyapatite [HAp, $Ca_{10}(PO_4)_6(OH)_2$] is one of the most attractive materials for bone implant due to its compositional and biological similarity to host materials. It has unique biocompatibility feature among phosphate groups. However, due to lower strength of pure HAp, it has been difficult to use it as bone implant for a long time. Mechanical strength of this material mainly depends on grain size, grain size distribution, porosity, and other microstructural defects. Bioactivity of the synthetic hydroxyapatite has been found to be strongly affected by structural crystallinity [1].

HAp powders have been synthesized using several methods including wet-chemical method in aqueous solutions [2], sol–gel method [3,4], hydrothermal method [5], thermal deposition [1] continuous precipitation [6], and solid state reaction method.

However, very few works have been reported on solid state reaction processing of HAp material, which can yield large amount using simpler processing. In this present work, synthesis and evaluation of HAp produced by solid state sintering reaction method using inorganic constituents have been undertaken.

Materials and Methods

To synthesize the synthetic hydroxyl-apatite (HAp), mostly inorganic oxides of calcium (CaO 50.52 wt%) and phosphorous (P_2O_5 46.43 wt %) and some small amount of other additives and binders were taken. These components were mixed in a ball mill [APEX make] for 16 hours followed by drying. This dried powder was compressed with varying of pressures (above 60 MPa) in a hydraulic machine [APEX make] into desired pellet shape and followed by sintering at round 1250^{o}C temperature for 1½ hours in a pit type furnace at the rate of 200^{o}C per hour**.** The non-stoichiometric Ca/P ratio 1.6 was obtained. For further improvement in properties, the sintered pellets were recrushed and resintered, after grinding and pelletization under similar conditions as mentioned above.

The phase identification of HAp was performed in X-ray Diffractometer (Seifert make, ISO Debyeflex-2002 model) using Cu-Kα radiation (λ=1.541838Å). The presence

of chemical bonding of HAp was also confirmed by Fourier transformation infrared (FTIR) analysis using FTIR spectrophotometer [Bruker make, Vector 22 model].

Surface morphology, particle size and its distribution, specific pore volume, specific particle surface area of the HAp samples were evaluated in scanning electron microscope [JEOL make, JSM 840A model] under 3,500x magnifications, BET analyzer (Beckman Coulter make, model SA 3100), and particle sizer analysette (Fritsch make, model 22). Pore volume and particle surface area were performed by Brunauer-Emmett-Teller (BET) surface area and pore size analyzer [Beckman Coulter, SA 3100 model].

Simulated body fluid (SBF) was prepared in laboratory by biocompatibility studies using several chemical compounds in specific proportions as shown in Table 1. A polished HAp sample was immersed in this SBF (as in Table 2) for 60 days. After the long immersion, samples were analyzed to surface roughness. Surface profiling for the above was performed using surface profilometer (Mitutoyo make, Model SJ 301).

Table 1: Typical Composition of Simulated Body Fluid (SBF)

Composition	Weight (gm) in one Liter Distilled Water
Sodium chloride (NaCl)	8.2187
Potassium chloride (KCl)	0.2260
Calcium chloride ($CaCl_2.2H_2O$)	0.3860
Sodium bi-carbonate ($NaHCO_3$)	0.3508
Di-Potassium hydrogen phosphate ($K_2HPO_4.3H_2O$)	0.3337
Sodium sulfate deca-hydrate ($Na_2SO_4.10H_2O$)	0.1697
Magnesium chloride hexa-hydrate ($MgCl_2.6H_2O$)	0.3366

Surface hardness measurement was performed in Vickers Microhardness Tester (Leitz make, Germany). Average hardness value was taken from at least five indents made for each sample and the maximum error obtained was found to be < 5%.

Mechanical characterization consists compressive, tensile and three point bending strengths. Universal testing machine or UTM (Hounsfield Test Equipment, England) was employed for these evaluations.

Results and Discussion

Hexagonal based crystal structure of the HAp materials was found by X-ray diffraction analysis shown in Fig 1 with lattice parameters of $a_o \cong 9.3852\pm0.05$ Å and $c_o \cong 6.8211\pm0.05$ Å. The XRD results of unsintered and sintered powders were found to be close to standard (File No. 9-432 in ICDD, JCPDS, 1985) values.

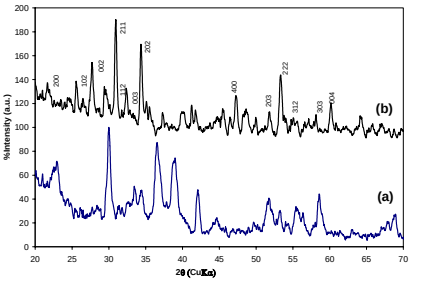

Figure 1: X-Ray Diffraction Pattern of HAp Specimens: (a) Apatite Powder Before Sintering; (b) Sintered Hydroxyapatite Powder.

The different phases were identified by complex calculation. The different crystal systems of the different phases with their major peaks are summarized in Table 2, which are supported by few reports [7,8,9].

Table 2: Phase Determination by X-RD Analysis for Un-sintered Apatite and Sintered hydroxyapatite Materials

Material	Sintering Temperature (^oC)	Crystal System	Major Peak at Angle (2θ)	Phase
(a) Apatite Powder	-	Hexagonal	30.04^o	Apatite
(b) Sintered Hydroxyapatite Powder	1250^oC	Hexagonal (a_o~9.3852±0.05Å and c_o~6.8211±0.05Å)	31.15^o, (211) plane	Hydroxyapatite

The FTIR spectroscopy for un-sintered apatite material (oxides mixtures) is shown in Fig 2. Characteristic FTIR curve of sintered (1250^{o}C) hydroxyapatite is given in Fig 3. Except sharp peak of 3570–3670 cm^{-1} corresponds to the stretching vibration of the lattice OH^{-} ions all peaks remain same as in Fig 2. This result says the hydrated O-H in the material decreases with increasing of sintering temperature [7,10]. Results getting from FTIR analysis are given as a tabular form in Table 3.

Table 3: Results of FTIR for HAp Before Sintering

Wave Number (cm^{-1})	Chemical Bonding for HAp Before Sintering
3670 – 3570	Sharp peak for stretching vibration OH^{-} ion
3500 –3100	Hydrated O-H
1250	Weak shoulder for P–O–H in plane
760 – 720	HPO_4^{2-} Weak peak out-of-plane
1090, 1040 – 1014, 950 – 937, 601 – 597, 570 – 558, and 470 – 420	PO_4^{3-}
635 – 628	Medium sharp peak for O–H bending deformation mode

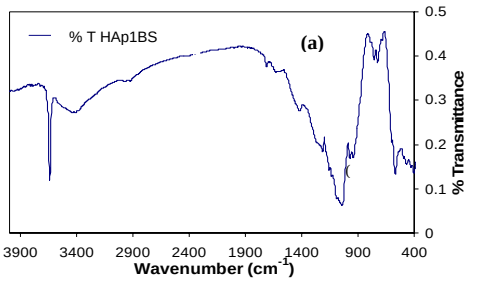

Figure 2: FTIR Spectrograph for apatite before Sintering

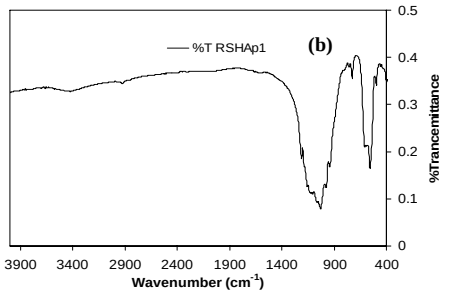

Figure 3: FTIR Spectrograph for Recrushed & Sintered Hydroxyapatite

The *in vitro* test for the recrushed sintered hydroxyapatite was performed using simulated body fluid (composition shown in Table 1). The polished sample was evaluated for surface roughness and then dipped in simulated body fluid for a long time of more than two months at room temperature. The surface roughness of the sample was measured again to evaluate the biocompability / chemical corrosion effect of body fluids on the material.

The polished Recrushed & Sintered HAp sample shows the roughness (Ra) of 0.77. The surface profile of this material is shown in Fig 4a. Prolong immersion of the same sample showed very little change in average surface roughness (Ra) which stands at 0.88. The surface profile of this tested material is shown in Fig 4b. Here, Ra is arithmetic mean deviation of the absolute values of the profile deviations from the mean line. The surface roughness parameters are summarized in Table 4.

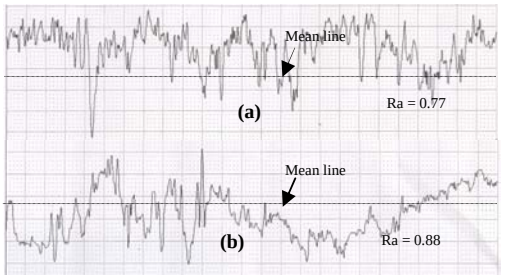

Figure4(a): Surface Profile of Polished Recrused & Sintered Hydroxyapatite (RSHAp135) before Immersion and (b) after Immersion in SBF (Scale: Vertical-2.0 µm/cm, Horizontal-200.0 µm/cm, and Traverse Length 2.5 mm)

Table 4: Surface Roughness Parameter (Ra) Before and After Immersion into the SBF

Roughness Parameter	Before Immersion	After 60 Days Immersion in SBF
Ra	0.77	0.88

Scanning electron microscopy observations exhibited considerable grain growth (3-11 µm) in sintered HAp materials (Fig 5).

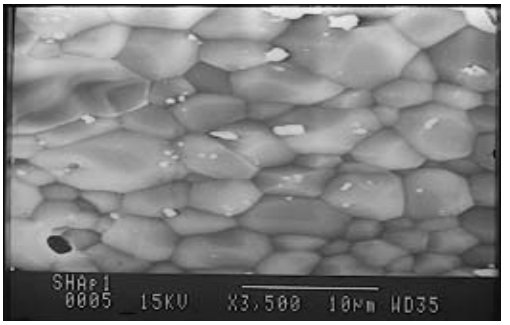

Figure 5: SEM Micrograph under x3500 magnification of sintered Hydroxyapatite (Compacted at 135 MPa, Sintered at 1250°C for 1½ Hour) [11]

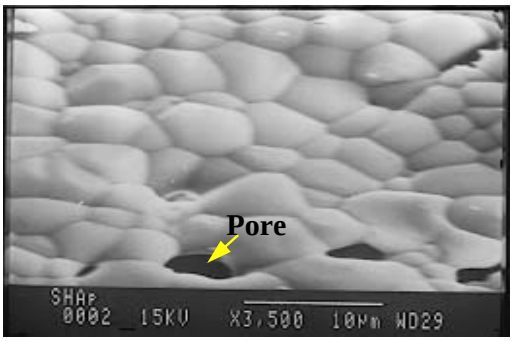

Figure 6: SEM Micrograph under x3500 magnification of recrushed & sintered Hydroxyapatite (Compacted at 135 MPa, Sintered at 1250°C for 1½ Hour) [11]

The scanning micrographs of recrushed & sintered HAp materials (in Fig 6) exhibited interlocked porous densed (1.98 gm/cc) structure of grain size 2-8 µm. Bulk density of the materials varies from 1.8 – 2.5 g/cc.

The variation of specific surface area ($[SpSA]_{particle}$) and pore volume ($[SpV]_{pore}$) as analyzed by BET technique also exhibited decreasing trend with increasing cold compaction pressure (CCP, is denoted by P_{CCP}) as shown in Table 5.

Table 5: Variation of Particles Specific Surface Area and Specific Pore Volume with Cold Compaction Pressure and both Strength and Modulus in Compression Varies with Specific Pore Volume

CCP (MPa)	Pore SpVol (cc/g)	Particle SpSA (sq.m/g)	CS (MPa)	Ec (GPa)
0	0.02164	1.981	0.002	0.000
46	0.00881	0.755	21.317	1.821
63	0.00623	0.54	34.116	4.463
135	0.00165	0.513	256.928	20.23

Average hardness of freshly produced sintered hydroxyapatite materials is 5.272 GPa (537.5 kgf/mm^2) which is similar to the reported [12,13] values. Vickers microhardness results of this measurement on the HAp and the femoral head bone are summarized in Table 6.

Table 6: Vickers Microhardness of HAp Material and Bone

Material	Average Vickers Hardness (GPa)	Average Vickers Hardness (kgf/mm^2)
Sintered hydroxyapatite	5.272	537.5
Recrushed & sintered hydroxyapatite (RSHAp135)	5.371	547.6
Cortical bone	0.396	40.4
Cancellous bone	0.345	35.2

Vickers micro-hardness of the product RSHAp135 is much larger that human femoral cortical bone. The cortical bone is 10 –15% harder than the adjacent cancellous bone. This difference is related to the calcium content of the two bone types [14]. The Vickers microhardness values improved with recrushing operation.

For compressive testing HAp samples with L/D ratio between 3 and 5 were used. Loads were applied with extension and compression rate of 0.01 mm/s. The experiment results are shown in Fig 7.

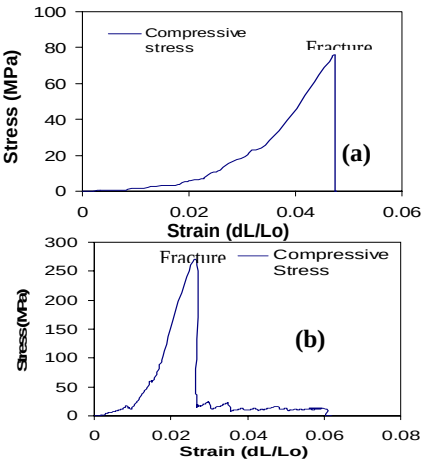

Figure 7: Compressive Stress – Strain Plots for (a) Sintered and (b) Recrushed & Sintered Samples

As reflected by Fig 7 the fracture strength of HAp material increases significantly after recrushing and sintering. The effect of increasing cold compaction pressure on Young's modulus in compression (Ec), compressive strength, tensile strength, and bending strength is shown in Table 8.

Table 8: Young's Modulus in Compression and Fracture Strength in Compression with various Cold Compaction Pressures (with a Constant Strain Rate of 0.01mm/s)

CCP (MPa)	E_C (GPa)	CS (MPa)
60	4.463	34.116
75	9.405	63.258
90	11.663	95.027
105	12.048	131.491
120	15.954	188.132
135	20.23	271.161

Conclusions

The experimental results of this study show that this large pored hydroxyapatite material has high strength and density very close range to that of actual femoral bone.

Increasing compaction pressure used for pelletization improves density as well as mechanical properties of HAp material.

Sample prepared after using recrushed powders from presintering gives significant improved properties and good biocompatibility.

The recrushed and sintered HAp has high resistance to surface reaction with the simulated body fluid.

References

1. Shi D, Jaing G, and Wen X, "in vitro Behavior of hydroxyapatite prepared by a Depositon Method", "in vitro Behavior of hydroxyapatite prepared by a Thermal Depositon Method", "Processing and Fabrication of Advanced Materials VIII," eds K. Khor et al. (World Scientific, Singapore), p. 117, 2001.

2. Kivrak N and Tas AC, "Synthesis of Calcium Hydroxyapatite-Tricalcium Phosphate Composite Bioceramic Powders and their Sintering Behavior", J. Am. Eram. Soc. **81**(9) (1998)2245-2252.

3. Balamurugan A, Kannan S, and Rajeswari S, "Bioactive Sol-Gel Hydroxyapatite Surface for Biomedical Application - invitro Study", Trends. Biomater. Artif. Organs, **16**(1)(2002)18-20.

4. Layrolle P, Ito A, and Tateishi T, "Sol–Gel Synthesis of Amorphous Calcium Phosphate and Sintering into Microporous Hydroxyapatite Bioceramics", J. Am. Ceram. Soc., **81** (6)(1998)1421–28.

5. Sivakumar M, Kumar TSS, Shantha KL, Rao KP, "Development of Hydroxyapatite Derived from Indian Coral", Biomaterials, **17**(1996)1709.

6. Tadic D and Epple M, "Mechanically Stable Implants of Synthetic Bone Mineral by Cold Isostatic Pressing", Biomaterials **24**(2003)4565–4571.

7. Koumoulidis GC, Vaimakis TC, and Sdoukos AT, "Preparation of Hydroxyapatite Lathlike Particles Using High-Speed Dispersing Equipment", J. Am. Ceram. Soc., **84**(6)(2001)1203–208.

8. Calderin L and Stott MJ, "Electronic and Crystallographic Structure of Apatites", Physical Review, **B67**, 134106(2003).

9. Yamashita K and Kanazawa T, "Hydroxyapatite"; Inorganic Phosphate Materials, Materials Science Monograph, Vol. **52**. p. 30, Edited by T. Kanazawa. Elsevier, *Tokyo, Japan, 1989*.

10. Nakamoto K, "Infrared and Raman Spectra of Inorganic and Coordination Compound", **4th** edition (1986), Wiley-Interscience publication, USA.

11. Pramanik S, "Development of Bioceramic Materials for Hip Joint Replacement", M. Tech Thesis, IIT Kanpur July 2004.

12. Ramesh S, "Grain Size – Properties Correlation in Polycrystalline Hydroxyapatite Bioceramic", Malaysian Journal of Chemistry, Vol. **3**(1) (2000)0035 – 0040.

13. Suchanek W, Yashima M, Kakihana M, and Yoshimura M, "Processing and Mechanical Properties of Hydroxyapatite Reinforced with Hydroxyapatite Whiskers", Biomaterials **17**(1996)1715-1723.

14. Bonser RHC, "Longitudinal Variation in Mechanical Competence of Bone along the Avian Humerus", The Journal of Experimental Biology **198**(1995)209–212.